J. Inst. Eng. India Ser. C (January–March 2016) 97(1):1–9
DOI 10.1007/s40032-015-0183-z

ORIGINAL CONTRIBUTION

Development and Experimental Study of Surface-Electrical Discharge Diamond Grinding of Al–10 wt%SiC Composite

Shyam Sunder Agrawal · Vinod Yadava

Received: 4 July 2013 / Accepted: 3 February 2015 / Published online: 21 February 2015

Abstract As silicon carbide possesses small fracture toughness, it is difficult to grind because it leads to cracking. Metal matrix composites can be machined using electrical discharge machining (EDM) but the process is slow. Electrical discharge diamond grinding (EDDG), which consists of diamond grinding and EDM with a rotating disk which enhanced material removal rate (MRR) and produce better surface finish. This paper describes the machining characteristic of Al–SiC composite using EDDG in surface grinding configuration which is called as surface-electrical discharge diamond grinding (S-EDDG). A chain of experiments were performed on S-EDDG set up by mounting newly self designed and fabricated set up on conventional die sinking EDM machine using the approach of one parameter-at-a-time concept. Surface roughness (R_a) and MRR are taken as output parameters as both are important outcome in the manufacturing process and they materialize a major division in the manufacturing system. The effects of current, wheel speed and depth of cut is analyzed on MRR and R_a. Finally, optimization have been done through weighted principal component analysis.

Keywords Surface-electrical discharge diamond grinding · Aluminum-metal matrix composites · Weighted principal component · Grinding · EDM

S. S. Agrawal (✉)
Mechanical Engineering Department, B. S. A. College of Engineering & Technology, Mathura 281004, Uttar Pradesh, India
e-mail: mtr_shyam@yahoo.co.in

V. Yadava
Mechanical Engineering Department, Motilal Nehru National Institute of Technology, Allahabad 211004, Uttar Pradesh, India

Introduction

Metal matrix composites (MMCs) materials are gaining abundant acceptance in applications where high specific strength, good elevated temperature properties and good wear resistance properties are required. MMCs are extensively used advanced engineering materials but their use is not escalating and not widespread adopted due to lack of appropriate machining techniques and it is a major impediment to commercially exploiting such materials. Full potential of these materials is hindered by high manufacturing cost involved, and difficulties in machining it. Particle reinforced aluminum alloy metal matrix composites have applications in various automotive and aerospace industries because of their enhanced properties compared with nonreinforced alloys [1–3].

Grinding of MMCs using conventional surface grinding process shows poor surface finish and accuracy [4]. Grinding of silicon carbide is difficult because of its low fracture toughness, making it very sensitive to cracking [5]. Electrical discharge machining (EDM) of MMCs containing electrically non conducting phases possess a few problems. The non conducting material particles hamper the process stability and impede the material removal process [6]. The results also show that aluminum–silicon carbide (Al–SiC) composite can be machined using EDM despite the low electrical conductivity and high thermal resistance of ceramic particle but the process is slow [7]. These problems can be taken care of in electrical discharge diamond grinding (EDDG) which is a hybrid machining process (HMP) comprising of diamond grinding (DG) and electrical discharge grinding (EDG). Material removal rate (MRR) is enhanced as the abrasive grains eradicate the non-conducting material particles, with spark discharges having thermally softened the surrounding binding material.

Hybrid processes of EDM and grinding is called as electro-discharge abrasive grinding (EDAG).When diamond grinding wheel is used in EDAG the process is termed as EDDG. In EDDG, the workpiece is subjected to simultaneous action of (i) abrasion action by abrasives of diamond wheel and (ii) erosion action by sparks generated between bonding material of wheel and workpiece. In case of EDG the material is removed only by electrical discharge, whereas, in case of EDDG, it is predominantly by abrasion, with the spark discharges playing more of a supportive role.

Material removal rate (MRR) is improved because diamond abrasive eliminates the particles, simultaneously spark discharges soften the surrounding binding material. There are three different modes on which EDDG can be operated. (1) cut-off-EDDG (C-EDDG). (2) face-EDDG (F-EDDG) (3) surface-electrical discharge diamond grinding (S-EDDG), through which plane surfaces can be machined by using peripheral surface of the wheel which rotates rotating about the horizontal axis.

Average surface roughness (R_a) produced on workpiece surface after machining is a key factor for evaluating machining performance and that is why, in many cases, industries are looking for maintaining the good surface quality of the machined parts. On the other hand, MRR, which indicates processing time of the workpiece, is another important factor that also greatly influences production rate and cost, so it is also necessary to study MRR with R_a in new configuration of EDDG which is termed as S-EDDG process. Both MRR and R_a greatly vary with change of process parameters. That is why proper selection of process parameters is also very essential for obtaining good surface quality (lower R_a value) and higher MRR in S-EDDG process.

Yadav et al. [8] showed the experimental analysis and design of process parameters during C-EDDG. Chandrasekhar et al. [9] performed experiments on face-electrical discharge grinding (F-EDG) set up. Singh et al. [10] conducted experiments for machining of tungsten carbide–cobalt (WC–Co) composite using F-EDDG process and determined setting of machining parameters.

Koshy et al. [11] did experimental work on the grinding of cemented carbide with electrical spark assistance, i.e., (C-EDDG). The results indicate that the discharges enhance the grinding performance by effectively declogging the wheel surface. Choudhary et al. [12] did experimental work on C-EDDG using high speed steel (HSS) (hardness 1200 HV, 5.6 mm wide) as work material. Experiments were conducted to find the effect of current, voltage, pulse on-time, and duty factor on MRR and grinding forces. Observations indicate that the normal grinding force decreases with increase in current, and trend reverses with increase in pulse on-time. MRR was found to be increasing with increasing current and pulse on-time, while the same decreases with increasing voltage and duty factor.

Singh et al. [13] conducted experiments for machining of WC–Co composite using F-EDDG process and determined setting of machining parameters. Furthermore, they also optimized machining parameters with multiresponse characteristics. Yadav et al. [14] did modeling and optimization of F-EDDG process on WC–Co composite using artificial neural network (ANN)-NSGA-II hybrid methodology. Srivastava et al. [15] presented modeling and simultaneous optimization of copper–iron–graphite composite on two important performance characteristics MRR and wheel wear rate (WWR) for the F-EDDG process. A hybrid approach of ANN, genetic algorithm, and grey relational was proposed for the optimization of different parameters. The verification results show considerable improvement in both performances.

From the discussed literature review, it has been concluded that most of experimental works related to EDDG have been done in cut-off grinding configuration (C-EDDG) and very little experimental work (Singh et al. only) has been conducted in face grinding configuration (F-EDDG). However, there has been no work done by authors till now in surface grinding mode of EDDG (S-EDDG). This paper analyze the effect on MRR and R_a during S-EDDG of Al–SiC workpiece due to current, wheel speed and infeed. A chain of experiments were done on newly self designed and fabricated set up attached to ZNC-EDM machine using the approach of one parameter-at-a-time concept.

Experimental Details

An attachment was developed and mounted on a Smart ZNC conventional die sinking EDM machine supplied by EMT, Ltd. Pune, India. The wheel is attached on electrical discharge machine with an attachment. Figure 1a shows schematic diagram of S-EDDG set-up and Fig. 1b shows dimension details of fabricated attachment attached to *Z*-axis replacing original tool holder of ZNC EDM machine. The rectangular workpiece was entirely dipped in dielectric liquid. Through belt pulley arrangement and with the help of variable-speed direct current (D.C.) motor the wheel was driven. The speed of the motor was varied by changing supply voltage with the help of a variac. The set up consists of D.C. motor, grinding wheel, V-belt, bearing, shaft and pulley. Here, shaft which is made from mild steel (MS) material is used and its diameter is 20 mm. The selected V-belt is having dimension 10 mm × 5 mm. Motor is indispensable component of the fabricated attachment which is situated 350 × 110 mm horizontal flat plate.

Since the experiment was to be performed in surface grinding mode, so an automatic table feed arrangement was made. The lead screw of the machine table was driven by

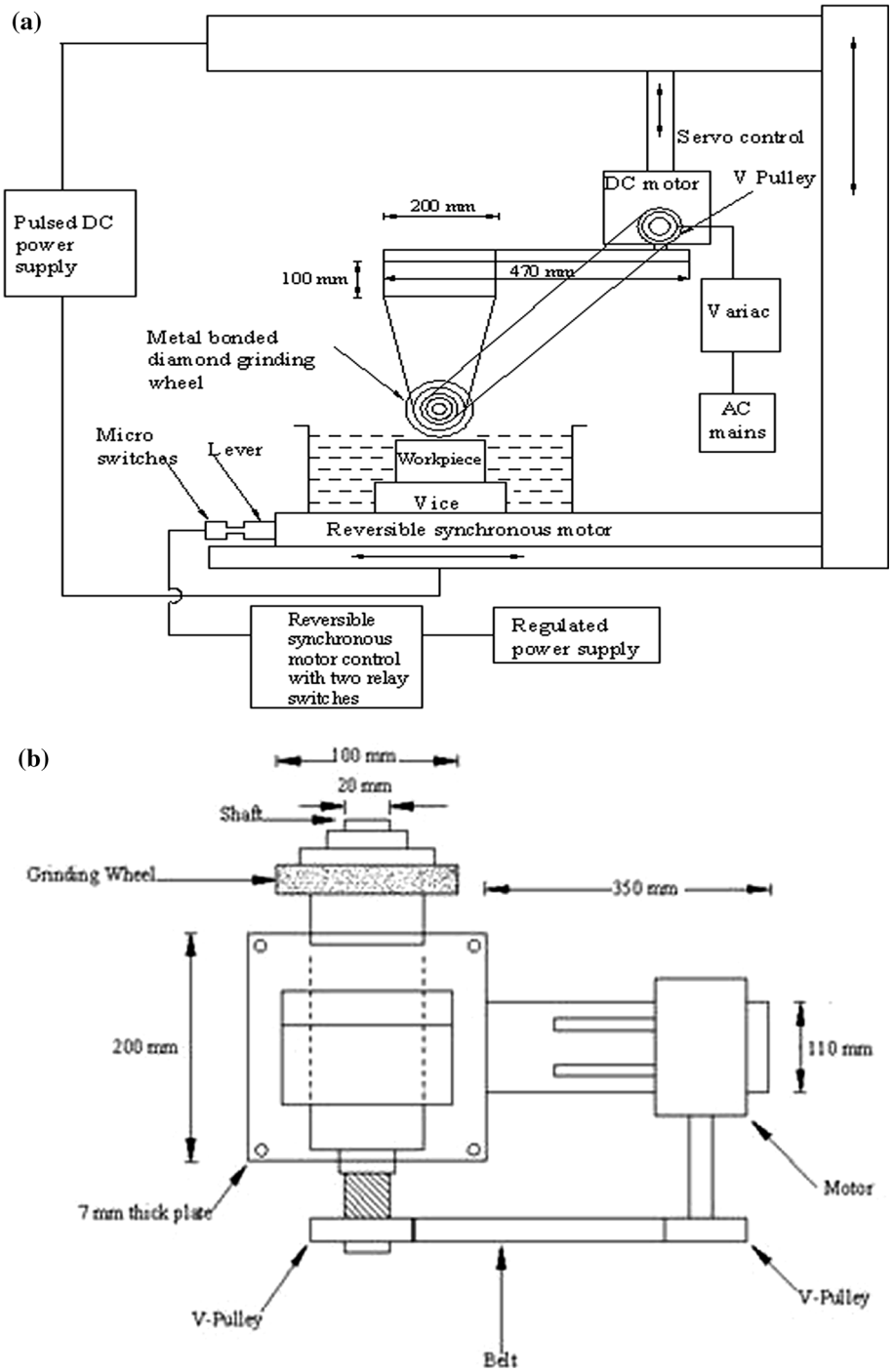

Fig. 1 **a** Schematic diagram of surface-electrical discharge diamond grinding set-up. **b** Dimension details of fabricated attachment attached to Z axis replacing original tool holder of EDM machine

reversible synchronous motor. Since for automatic to and fro motion of the table motor should automatically revolve both in anticlockwise and clockwise direction as and when required, therefore a reversible synchronous motor control circuit was designed using two limit switches, relay switch, regulated power supply and voltage regulator for controlling the table speed. Working of this automatic control is very simple. Suppose the motor is revolving in clockwise direction and as a result, table is moving in forward direction. When a lever attached to machine table presses the limit switches, polarity of the reversible synchronous motor will automatically changed and motor start to rotate in anticlockwise direction and therefore table will move in reverse direction. Figure 2 shows the real snaps of the developed setup on EDM machine.

Before study the effect of current, wheel speed and in-feed on MRR and R_a a lot of pilot experiments had been performed for deciding the range of input process

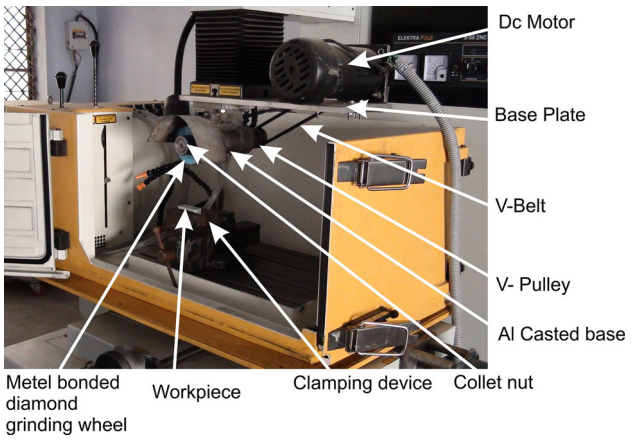

Fig. 2 EDSG set up assembled on EDM machine

parameters. During it one factor has been changed while other factors remain constant in each set. The range of process parameter for machining Al–SiC composite was selected: 1000–1400 wheel rotation per min (RPM), 8–24 A pulse current, 0.492–0.817 duty factor, 50–150 μs pulse on-time, 20–40 μm infeed and table speed 3–5 mm/sec. For less than 8 A current it is seen that MRR is too low and surface roughness increases for more than 24 A current. The range for pulse on-time was usually used for the EDDG. Levels of duty factor is selected which cover up wide range. The wheel speed and table speed selected as per the robustness and design of fabricated attachment. The size of the SiC particles was of 20 μm. EDM fluid supplied by EMT Ltd. Pune, India, is used as a dielectric in which major portion consist of paraffinic hydrocarbon oil. Experiments were performed on rectangular workpiece made of Al–SiC composite. R_a of each machined workpiece has been measured by Talysurf surtronic 25 whose cutoff value is 0.8.

Experimental Study of S-EDDG

After experimentation on S-EDDG the effect of current, wheel speed and infeed on MRR and R_a is reported in S-EDDG of Al–SiC MMC.

Effect of Current

Figure 3a explains the how MRR varies with pulse current for different value of duty factor. Here, pulse on-time 100 μs, wheel speed 1200 RPM, infeed 30 μm and table speed 4 mm/sec were taken. From graph, it is concluded that for any value of duty factor within range MRR raises with rising in current. The reason behind is that when pulse current rises more energy is liberated and grinding action is dominated by EDM. It is also concluded that for current

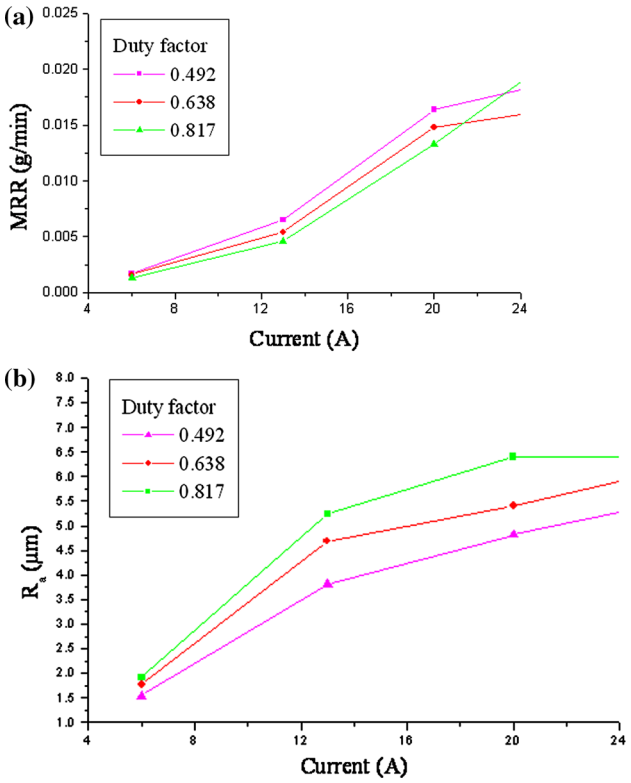

Fig. 3 **a** Effect of current on MRR for different duty factor (wheel speed = 1200 RPM, pulse on-time = 100 μs, infeed = 30 μm, table speed = 4 mm/sec). **b** Effect of current on R_a for different duty factor (wheel speed = 1200 RPM, pulse on-time = 100 μs, infeed = 30 μm, table speed = 4 mm/sec)

within range MRR rises with reduce in duty factor. It is a well-known fact that increasing the duty factor for constant pulse on-time lowering will be the off-time. Off-time is responsible so that there is proper restoration of insulation between the gap and simultaneously at the end of every pulse; it de-ionizes the dielectric so that machining process become stable. If adequate pulse off-time is there it may have well time to remove the particles from inter electrode gap (IEG), so arcing does not took place consequently MRR increases.

Figure 3b shows the variation of current on abscissa and variation of R_a on ordinate for duty factor of 0.492, 0.638 and 0.817. For a particular current R_a increases with the increase of duty factor, because increasing in the duty factor for a particular pulse on-time means lesser pulse off-time. Basically, in on-time, a material becomes melted and off-time is responsible for removal of melted materials and it comes out from IEG. At a particular pulse on-time, larger duty factor, means smaller pulse off-time which hampers the suitable discharge of this molten material, follow on an increase R_a due to the formation of the resolidified layer.

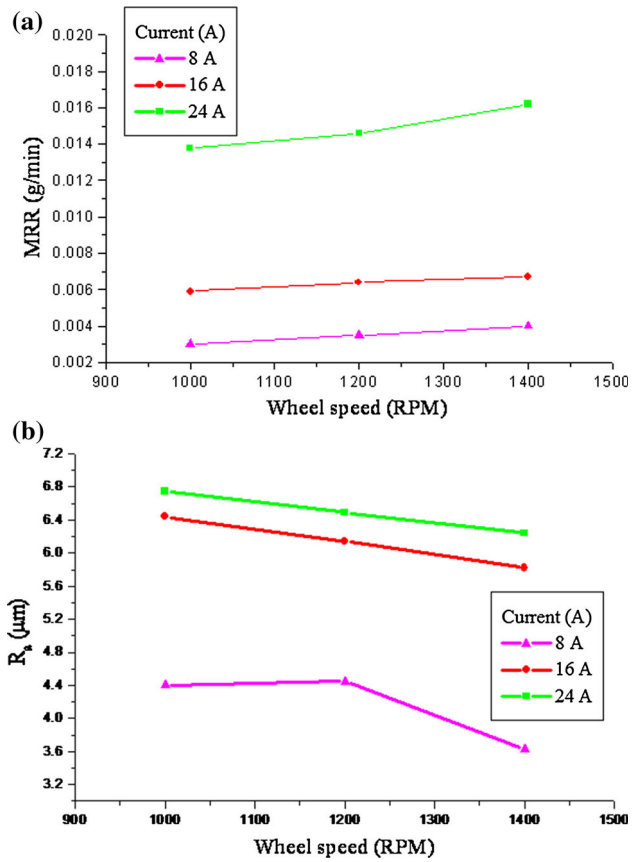

Fig. 4 **a** Effect of wheel speed on MRR for different current (pulse on-time = 100 µs, duty factor = 0.638, infeed = 30 µm, table speed = 4 mm/sec). **b** Effect of wheel speed on R_a for different current (pulse on-time = 100 µs, duty factor = 0.638, infeed = 30 µm, table speed = 4 mm/sec)

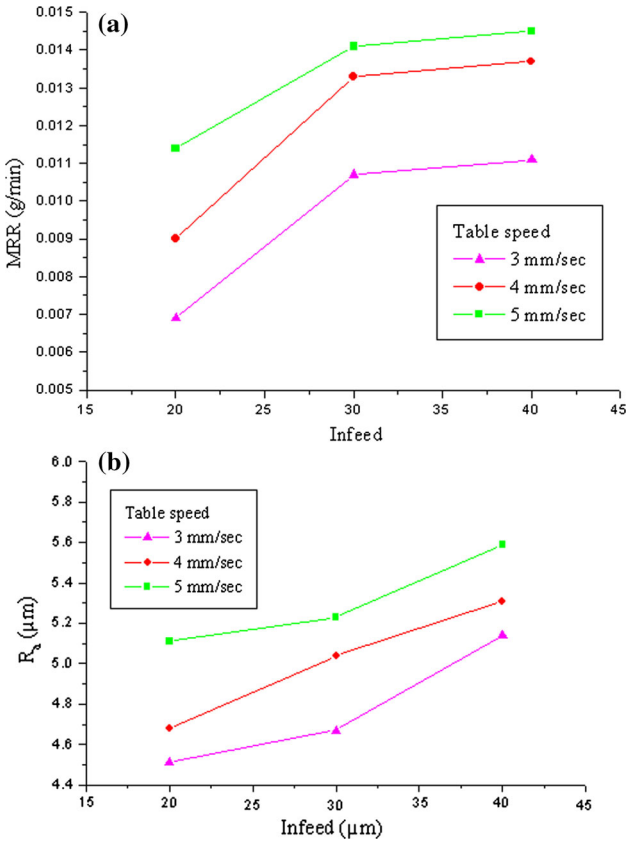

Fig. 5 **a** Effect of infeed on MRR for different table speed (pulse on-time = 100 µs, duty factor = 0.638, wheel speed = 1200 RPM, current = 16 A). **b** Effect of infeed on R_a for different table speed (pulse on-time = 100 µs, duty factor = 0.638, wheel speed = 1200 RPM, current = 16 A)

Effect of Wheel Speed

In Fig. 4a abscissa shows variation of wheel RPM while ordinate shows variation of MRR for currents of 8, 16 and 24 A. It can be clearly observed that for any fixed value of wheel RPM raising the current leads to more heat conduction to workpiece causing more material to be thermally softened resulting to more material removal by grinding action as well as discharge action. Further, it is clearly seen that for any particular value of current MRR increases with increasing wheel RPM. The reason might be that when RPM increases, gap current flow increases with the help of spark discharges through the grinding region due to which MRR increases. Also, for given discharge energy that is for a particular on-time and current, melted material is being quickly thrown away form this operational gap as wheel RPM increases. Also, for higher wheel RPM there is better dielectric flushing.

Figure 4b shows the variation of R_a with wheel speed for different current value fall within range. Here, pulse on-time 100 µs, duty factor 0.638, infeed 30 µm, table speed 4 mm/sec was taken. Here it can be clearly seen that for every current values R_a decreases with rise in wheel RPM. As wheel RPM increases there is better and effective flushing of IEG occurs due to high speed of wheel and therefore possibilities that particles becomes resolidify on the workpiece is reduced and as a result surface roughness decreases. It has been also observed that R_a rises with rising in current for within range of wheel RPM. The reason may be most likely that craters will be produced on workpiece surface due to which it leads to higher R_a.

Effect of Infeed

In Fig. 5a, abscissa shows variation of infeed and ordinate shows variation of MRR for different table speed. Here 100 µs, pulse on-time, 0.638 duty factor, 1200 wheel RPM, and 16 A current was taken. For infeed, MRR increases with feed rate. For fixed infeed, with increasing feed rate machining time reduces consequently MRR increases. MRR also increases as infeed increases.

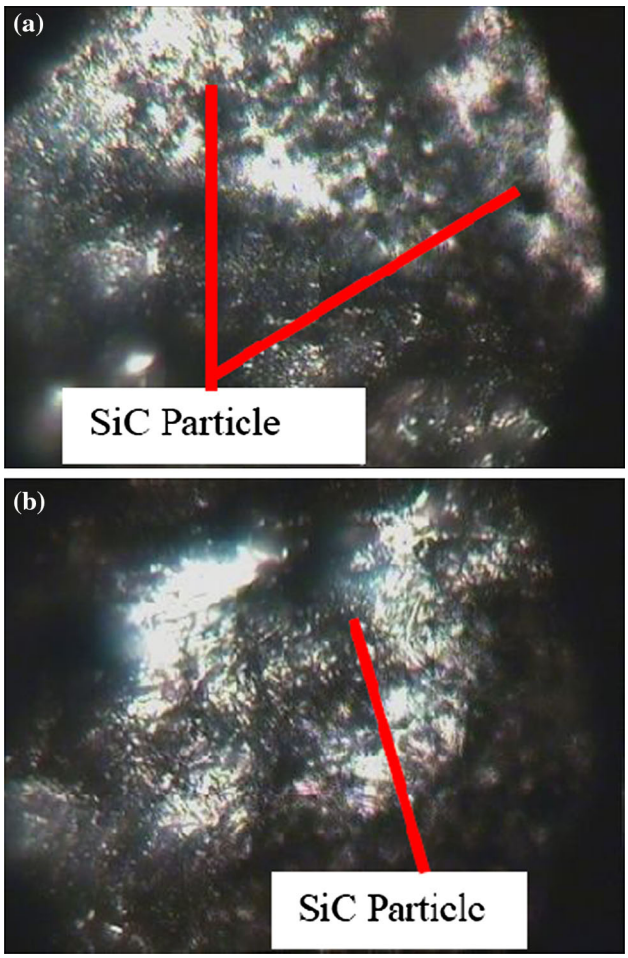

Fig. 6 Micro graphs of work surface after Surface-EDDG, **a** infeed = 10 μm, **b** infeed = 30 μm (wheel speed = 1200 RPM, duty factor = 0.638, pulse on-time = 100 μs, table speed = 4 mm/sec)

Figure 5b shows variation of infeed on abscissa and variation of R_a on ordinate for different table speed. Here 100 μs pulse on-time, 0.638 duty factor, 1200 wheel RPM, 16 A current was taken. It may be seen that for a particular infeed R_a increases with feed rate because with at increased feed rate possibilities of resolidification particles becomes high due to high speed of worktable and there is not adequate time to remove the particles from the IEG and hence R_a increases. It is also observed that R_a rises with rising infeed. The possible reason might be that with increasing depth, percentage area of surface damage increases. The other reason might be that as infeed increases there is increment in number of silicon carbide (SiC) particles which are covered by aluminum matrix and now that are pulled out from the surface, consequently the roughness of workpiece increases. Figures 6a, b show micrographs at different infeed which shows that more SiC particles are pulled out at greater infeed which increases the roughness at greater depth.

Table 1 Experimental observations for Al–SiC composite using L_{18} OA

S.no	Factor level						MRR (g/min)	R_a (μm)
	S	C	T	DF	V_w	d		
1	1	1	1	1	1	1	0.0082	3.01
2	1	2	2	2	2	2	0.0109	6.26
3	1	3	3	3	3	3	0.0213	7.09
4	2	1	1	2	2	3	0.0127	5.47
5	2	2	2	3	3	1	0.0134	5.02
6	2	3	3	1	1	2	0.0179	4.54
7	3	1	2	1	3	2	0.0160	5.71
8	3	2	3	2	1	3	0.0138	5.47
9	3	3	1	3	2	1	0.0365	4.66
10	1	1	3	3	2	2	0.0130	5.56
11	1	2	1	1	3	3	0.0101	6.05
12	1	3	2	2	1	1	0.0118	3.97
13	2	1	2	3	1	3	0.0124	6.46
14	2	2	3	1	2	1	0.0344	6.50
15	2	3	1	2	3	2	0.0280	5.02
16	3	1	3	2	3	1	0.0264	4.99
17	3	2	1	3	1	2	0.0356	5.29
18	3	3	2	1	2	3	0.0337	6.34

Table 2 The explained variation and eigenvectors

Principal components	Eigen value	Explained variation	Cumulative variation	Eigen vector
Z_1	1.1788	58.94	58.94	[0.707, 0.707]
Z_2	0.8212	41.06	100.00	[0.707, −0.707]

Optimization of S-EDDG Using Weighted Principal Component Analysis (WPCA)

The detail analysis regarding WPCA has been given in [16]. In the present case, authors have considered six parameters at three different levels assuming no interaction between them then total degree of freedom (dof) has been calculated as:

$$\text{dof} = (3-1) \times 6 + 1 = 13$$

Hence, a standard L_{18} orthogonal array (OA) was taken for experimentation. The experiments are performed as per standard L_{18} OA (Table 1). Table 2 shows the explained variation in these responses and eigenvector of each principal component.

Relations between principal components and responses are:

$$Z_1 = 0.707 \times MRR + 0.707 \times R_a, \text{ and}$$
$$Z_2 = 0.707 \times \text{MRR} + (-0.707) \times R_a$$

Table 3 Calculated multi-response performance index

S.No	Factor Level						MPI
	S	C	T	DF	V_w	d	
1	1	1	1	1	1	1	0.1264
2	1	2	2	2	2	2	0.0932
3	1	3	3	3	3	3	0.3271
4	2	1	1	2	2	3	0.1626
5	2	2	2	3	3	1	0.1940
6	2	3	3	1	1	2	0.3213
7	3	1	2	1	3	2	0.2376
8	3	2	3	2	1	3	0.1900
9	3	3	1	3	2	1	0.7822
10	1	1	3	3	2	2	0.1673
11	1	2	1	1	3	3	0.0796
12	1	3	2	2	1	1	0.1865
13	2	1	2	3	1	3	0.1243
14	2	2	3	1	2	1	0.6727
15	2	3	1	2	3	2	0.5587
16	3	1	3	2	3	1	0.5203
17	3	2	1	3	1	2	0.7402
18	3	3	2	1	2	3	0.6602

The equation of WPC, multiple performance index (MPI), is

$$\text{MPI} = 0.5894 \times Z_1 + 0.4106 \times Z_2$$

Table 3 shows the obtained MPI value in the standard array L_{18}.

The main effects of each control factor on MPI are given in Table 4. Basically, the larger is the MPI the smaller is the variance of the performance characteristic. The use of MPI to perform the analysis of variance (ANOVA) analysis is shown in Table 5. Wheel speed and current are the most significant process parameters for affecting the multiple quality characteristic. From the response table shown in Table 4, the best combination of input parameters is the set with $S_3C_3T_1DF_3V_{w2}d_1$ i.e., wheel speed at 1400, current at 24 A, pulse on-time 50 µs, duty factor 0.817, table speed 4 mm/sec, infeed 20 µm. The percentage contribution of each control factor to the total variance is wheel speed 46.36 %, current 22.66 %, pulse on-time 9.80 %, duty factor 3.97 %, table speed 6.47 % and infeed 10.76 %. Table 6 shows the comparison of experimentally obtained MRR and R_a at optimum S-EDDG process parameters with initial parameter setting. Three confirmation experiments were conducted by using the optimal parameter

Table 4 Response table for multi-response performance index

Symbol rank	Machining parameter	MPI			Effect	Rank
		Level 1	Level 2	Level 3		
S	Wheel speed	0.1634	0.3389	0.5218	0.3584	1
C	Current	0.2231	0.3283	0.4727	0.2496	2
T	Pulse on-time	0.4083	0.2493	0.3665	0.1590	4
DF	Duty factor	0.3496	0.2852	0.3892	0.1040	5
V_W	Table speed	0.3004	0.3740	0.3374	0.0736	6
d	Infeed	0.4711	0.3215	0.2433	0.2278	3

Table 5 Result of ANOVA

Symbol	Machining parameters	SS	dof	Variance	F	PC (%)
S	Wheel speed	0.38540	2	0.19270	8.89#	46.36
C	Current	0.18841	2	0.09221	4.25	22.66
T	Pulse on-time	0.08150	2	0.04075	1.87	9.80
DF	Duty factor*	0.03305	2	–	Pooled	3.97
V_w	Table speed*	0.05366	2	–	Pooled	6.45
d	Infeed	0.08940	2	0.0447	2.06	10.76
Pooled error		0.08671	4	0.021678		
Total		0.83142				100

* Pooled factors, tabulated F-ratio at 95 % confidence level: $F_{0.05;\ 2,4} = 6.94$

Significant at 95 % confidence level

Table 6 Results of confirmation experiment

	Initial parameter Setting	Optimal S-EDDG machining parameters Experiment
Level	$S_1C_1T_1DF_1V_{w1}d_1$	$S_3C_3T_1DF_3V_{w2}d_1$
MRR (g/min)	0.0082	0.0371
R_a (μm)	3.01	4.61

combination. The average value of MRR, and R_a at optimum level were found to be 0.0371 g/min, and 4.61 μm. It can be seen that the performance of S-EDDG process has been improved. Though the improvement in MRR is quiet significant (up to 352 %), surface roughness has been increased from 3.01 to 4.61 μm.

Discussion on Results Observed

Folowing discussions have been obtained after carefully observations of the results.

1. It was also observed that MRR was found to be increased five times and surface roughness is reduced to almost half when wheel speed is varied between 1000 and 1400 wheel speed under the range of current investigated. For infeed range 20–40 μm with increase in table speed (3–5 mm/sec) the MRR increases by a factor of 2.2. At 24 A, MRR becomes almost same for duty factor ranging from 0.492 to 0.817. For a infeed range 20–40 μm, and for table speed (3–5 mm/sec) the roughness increases up to 45 % and there is significant improvement in roughness at higher speed as compared to lower speed due to improper flushing.
2. The micrographs examination indicated that the machining surface at higher current influenced by electro-erosion and dielectric flushing effect as compare to low current at same parameters settings.
3. The micrographs indicate that there is no recast layer in S-EDDG process during machining of composite materials which has been found when process behaves in EDM mode.
4. It was evident from the above study that optimization of the complicated multiple-performance characteristics can be greatly simplified through WPC. It is shown that the performance characteristics of the S-EDDG process such as MRR and R_a are improved together by using the method proposed by this study. The effectiveness of this approach has been successfully established by validation experiment. Whereas improvement in MRR is 352 %, R_a deteriorates up to 34.70 % from their initial setting during S-EDDG while performing simultaneous optimization of multiple quality characteristics.

Conclusions

The combination of EDM and diamond surface grinding (DSG) improves the MRR and R_a that is machining performance in terms of output process parameters during S-EDDG of MMCs which was alone not possible from EDM and grinding. An experimental set up for EDDG process for a new configuration of surface grinding mode has been developed. Experiments were conducted to study the effect of current, pulse on-time, wheel speed, duty factor on MRR and R_a. The following conclusions are drawn after carefully observations of the results.

1. To achieve better surface finish on the workpiece surface lower value of pulse current, duty factor, pulse on-time, infeed, table speed and higher value of wheel speed should be selected. R_a value varies from 1.5 to 6.5 μm, for most of experimental conditions used.
2. For higher MRR pulse current, wheel speed, pulse-on time, infeed, table speed should be selected from their high ranges and duty factor from lower range. MRR value varies from 0.001 to 0.0190 g/min for most of the conditions used.
3. The factors setting found as best combination of process variables is: wheel speed-level 3 (1400), table speed-level 2 (4 mm/sec), infeed-level 1 (20 μm), current- level 3 (24 A), pulse on-time- level 1 (50 μs) and duty factor-level 3 (0.817).The percentage contribution of different factors in decreasing order is wheel speed 46.36 %, current 22.66 %, infeed 10.76 %, pulse on-time 9.80 %, table speed 6.45 % and duty factor 3.97 %. With in all input parameters considered, wheel speed parameter has the maximum effect on S-EDDG process which has also been confirmed by that fact that its significancy level is more than 95 % which has been observed from Table 5.

References

1. F. MÜller, J. Monaghan, Non-conventional machining of particle reinforced metal matrix composites. Int. J. Mach. Tools. Manuf. **40**, 1351–1366 (2000)
2. A. Manna, B. Bhattacharayya, A study on machinability of Al/SiC-MMC. J. Mater. Process. Technol. **140**, 711–716 (2003)
3. S. Kannan, H.A. Kishawy, I.M. Deiab, M.K. Surappa, On the role of reinforcements on tool performance during cutting of metal matrix composites. J. Manuf. Process. **8**(2), 67–75 (2006)

4. P.R. Aguair, F.R.L. Dotto, E.C. Bianchi, Study of thresholds to burning in surface grinding process. J. Braz. Soc. Mech. Sci. Eng. **27**(2), 150–156 (2005)
5. A.V. Gopal, P.V. Rao, Selection of optimum conditions for maximum material removal rate with surface finish and damage as constraints in SiC grinding. Int. J. Mach. Tools Manuf. **43**, 1327–1336 (2003)
6. W. Koing, D.F. Dauw, G. Levy, U. Panteen, EDM-future steps towards the machining of ceramic. Ann. CIRP **37**(2), 623–631 (1998)
7. F. MÜller, J. Monaghan, Non-conventional machining of particle reinforced metal matrix composites. J. Mater. Process. Technol. **118**, 278–285 (2001)
8. S.K.S. Yadav, V. Yadava, V.L. Narayana, Experimental study and parameter design of electro-discharge diamond grinding. Int. J. Adv. Manuf. Technol. **36**, 34–42 (2008)
9. B. Chandrasekhar, V. Yadava, G.K. Singh, Development and experimental study of electro-discharge face grinding. Mater. Manuf. Process. **25**(6), 1–6 (2010)
10. G.K. Singh, V. Yadava, R. Kumar, Diamond face grinding of WC-Co composite with spark assistance: experimental study and parameter optimization. Int. J. Precis. Eng. Manuf. **11**(4), 509–518 (2010)
11. P. Koshy, V.K. Jain, G.K. Lal, Grinding of cemented carbide with electrical spark assistance. J. Mater. Process. Technol. **72**, 61–68 (1997)
12. S.K. Choudhary, V.K. Jain, M. Gupta, Electrical discharge diamond grinding of high-speed steel. Mach. Sci. Technol. **3**(1), 91–105 (1999)
13. G.K. Singh, V. Yadava, R. Kumar, Multi response optimization of electro-discharge diamond face grinding process using robust design of experiments. Mater. Manuf. Process. **25**(1), 1–6 (2010)
14. R.N. Yadav, V. Yadava, G.K. Singh, Application of ANN-NSGA-II hybrid methodology for modeling and optimization of electrical discharge diamond face grinding of tungsten carbide-cobalt (WC-Co) composite. J. Mach. Form. Tech. **4**, 3–4 (2012)
15. P. Srivastava, A.K. Dubey, Intelligent modeling and multi-objective optimization of electric discharge diamond grinding. Mater. Manuf. Process. **28**(9), 1036–1041 (2013)
16. H.C. Liao, Multi-response optimization using weighted principal component. Int. J. Adv. Manuf. Technol. **27**, 720–725 (2006)